

High Beta Discharges with Hydrogen Storage Electrode Biasing in the Tohoku University Helic

Hiroyasu UTOH, Kiyohiko NISHIMURA¹⁾, Hajime UMETSU, Keiichi ISHII, Shigeru INAGAKI²⁾, Masayuki YOKOYAMA¹⁾, Yasuhiro SUZUKI¹⁾, Hiromi TAKAHASHI¹⁾, Yutaka TANAKA³⁾, Atsushi OKAMOTO, Takashi KOBUCHI, Sumio KITAJIMA and Mamiko SASAO

Department of Quantum Science and Energy Engineering, Tohoku University, Sendai, 980-8579, Japan

¹⁾*National Institute for Fusion Science, Toki 509-5292, Japan*

²⁾*Research Institute for Applied Mechanics, Kyushu University, Fukuoka 816-8580, Japan*

³⁾*Japan Atomic Energy Agency, Naka 311-0193, Japan*

(Received: 4 September 2008 / Accepted: 21 November 2008)

In the Tohoku University Helic (TU-Helic), high-beta-discharge experiments were done with hydrogen storage electrode biasing by varying the magnetic configurations and the magnetic field. High-beta plasma was produced in the magnetic well and hill configurations (the magnetic well depth at the last closed flux surface (LCFS) were 3.3 % and -1.6 %) at the magnetic field on axis $B_0 = 0.075$ T with hydrogen storage electrode biasing. The electron density increased within a short time, and this density increment was degraded. In both the magnetic well and hill configurations, this density increment was observed; however, the rates of increase and decrease in the well and hill configurations were different. When short-term high-pressure plasma was produced in the magnetic well configuration, the local beta value was the highest, about 5-fold that before biasing. The fluctuations of ion saturation current observed at the electrode biasing differed between the well and hill configurations. These results suggest that the high-beta plasma produced by hydrogen storage electrode biasing depends on the magnetic configuration, and the degradation of high-beta plasma was triggered by MHD instability caused by the rise in the beta value.

Keywords: helic, electrode biasing, particle injection, high-density, high-beta

1. Introduction

In stellarators, there is no hard limit for high-density operation, unlike the Greenwald density limit in tokamaks; this is one of their great advantages for future reactor operation. Therefore, it is important to study high-density plasma production and to explore the high-density operation of stellarators. In addition, the Tohoku University Helic (TU-Helic) has a non-planar magnetic axis system, which is expected to confine high-beta plasma due to the self-stabilization effect [1-3].

In our previous experiments on the TU-Helic, the role of the radial electric field on the transition to improved modes was investigated by electrode-biasing experiments. In negative biasing experiments with a hot cathode electrode (electron-emission), the radial electric fields could be actively controlled by changing the electrode current, I_E [4-6].

Consequently, a new type of electrode made of hydrogen storage metal has been developed for particle injection (electrons, ions and neutral particles). Using an electrode made of a hydrogen storage metal, such as

titanium (Ti) or vanadium (V), it can be expected that (1) the injection of electrons from the negative-biased electrode enables biasing experiments for the study of LH transition by control of the electrode current, (2) the injection of electrons/neutral particles from the negative-biased electrode produces high-beta plasma and high-density plasma, and (3) the acceleration of ions from the positive-biased electrode would allow for simulation of the orbit loss of high-energy particles, if hydrogen could be stored successfully in the electrode and released from the electrode. In the TU-Helic, the highest density has been about $1 \times 10^{19} \text{ m}^{-3}$, achieved by pre-filling working gas. The discharge time (10 ms) is not sufficient to increase the plasma density by additional gas puffing. By contrast, bias electrodes made of hydrogen storage metals can increase the density at the plasma core rapidly (< 0.5 ms) like a pellet injection. Actually, in the TU-Helic, high-density plasma was produced ($> 10^{19} \text{ m}^{-3}$) using a titanium (Ti), vanadium (V) or gold (Au)-coated palladium (Pd-Au) electrode after the hydrogen gas charging in negative electrode biasing [7-9]. Specifically, when a V or Pd-Au electrode was

negatively biased in an Ar plasma under a low magnetic field in the standard operation, the beta value increased up to about 0.5 %, allowing the realization of a new field of high-beta experiments. Negative biasing experiments using a hydrogen storage electrode have the potential to realize high-beta experiments in some small-sized devices.

In the present work, we show high-pressure and high-beta-discharge experiments with hydrogen storage electrode biasing by varying the magnetic configurations and the magnetic field.

2. Experimental setup

2.1. TU-Heliac

The TU-Heliac is a small standard heliac device (major radius $R = 0.48$ m, average plasma radius $a = 0.06$ m) with the toroidal magnetic period $n = 4$ [10, 11]. The heliac configurations are produced by three sets of coils: toroidal field coils, a center conductor coil, and vertical field coils. Various magnetic configurations can be formed easily by selecting the ratios of coil currents, and Fourier components of the magnetic field can be varied over a wide range. Therefore, the heliac configuration has the flexibility of a rotational transform and the depth of a magnetic well. It is useful to confirm the beta value dependence on the configuration in the heliac. The target plasma was produced by Ohmic heating with an 18.8 kHz alternating current in additional poloidal coils, with the effective input power of about 3 kW. The vacuum vessel was filled with a working gas (Ar) before discharge. The magnetic field on the axis, B_0 , was 0.3 T in the standard operation. We selected three magnetic configurations. Figure 1 shows the radial profiles of the magnetic well depth and the rotational transform in configurations (a)-(c). Configuration (b) was the standard configuration at TU-Heliac. The magnetic well depth at the last closed flux surface (LCFS), and the rotational transform at the

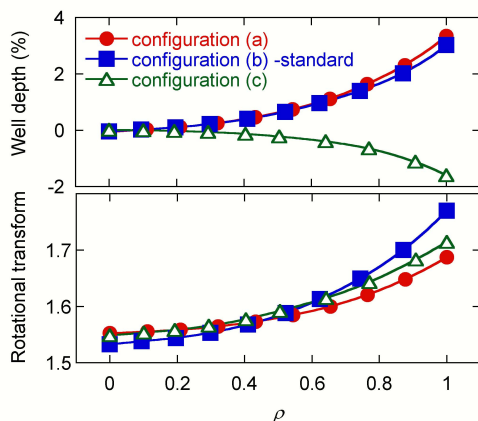


Fig. 1 Radial profiles of the magnetic well depth and the rotational transform in configurations (a)-(c). Configuration (b) was the standard configuration of the TU-Heliac.

magnetic axis were 3.0 %, and 1.77, respectively. Configurations (a) and (c) had high or low magnetic well depths compared to that of configuration (b); the magnetic well depths at LCFS were 3.3 %, and -1.6 %, respectively. Configurations (a) and (c) had an average minor radius a of ~ 0.04 m, and had almost the same rotational transforms of ~ 1.7 . In this paper, configurations (a) and (c) were used for high-beta-discharge experiments with hydrogen storage electrode biasing at the magnetic fields on axis $B_0 = 0.3$ T, 0.150 T, and 0.075 T.

High-speed fluctuation measurement and triple probe measurements were integrated in a high-speed triple probe (HSTP). This system measures electron density, n_e , electron temperature, T_e , floating potential, V_f , and plasma space potential, V_s , radially across the magnetic axis at toroidal angle $\phi = 0^\circ$ [12, 13]. The electron line-density, $n_e l$, was measured with a 50-GHz microwave interferometer at $\phi = 90^\circ$.

2.2. Hydrogen storage electrode

The experimental set-up of the hydrogen storage electrode is shown in fig. 2 together with the cross-section of the vacuum magnetic flux surfaces at toroidal angle $\phi = 0^\circ$. In these experiments, gold (Au)-coated palladium (Pd-Au) was used as the hydrogen storage electrode. An electrode made of Pd-Au was inserted into the plasma, vertically from the top at $\phi = 0^\circ$. It was biased positively or negatively against the vacuum vessel through a field-effect transistor (FET). The hydrogen storage electrode head (10 mm in diameter and 2 mm in length) was mounted at the end of a copper shaft housed in a glass tube as an insulating sheath. The

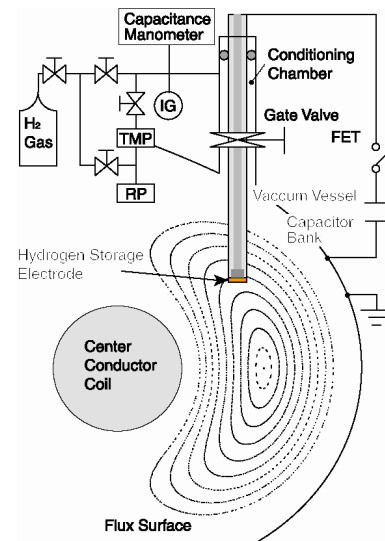


Fig. 2 The position of the hydrogen storage electrode and the computed cross-section of the vacuum magnetic flux surfaces at $\phi = 0^\circ$. The hydrogen storage electrode (10 mm in diameter and 2 mm in length) was inserted vertically into the plasma from the low-magnetic-field side.

hydrogen storage electrode was conditioned in the upper chamber (conditioning chamber) separated by a gate valve. The temperature of the hydrogen storage metal head was measured with a thermocouple gauge installed inside the electrode head.

3. Experimental results

After baking, the gold (Au)-coated palladium electrode was conditioned in hydrogen gas ($p_{\text{in}} = 26.7$ kPa) at room temperature. The decrease in hydrogen gas pressure p_{in} in the Pd-Au electrode Δp_{in} was 6.0 kPa. The number of Pd atoms in the electrode, $N_{\text{Pd-Au}}$, was 1.5×10^{22} , and the total number of hydrogen atoms absorbed in the Pd-Au electrodes was estimated from the decrease in hydrogen gas pressure after treatment, equivalent to about 2.4×10^{21} hydrogen atoms (N_{H}); the hydrogen concentration in the Pd-Au electrode ($x = N_{\text{H}} / N_{\text{Pd-Au}}$) was about 0.16.

In standard configuration (b), by negative biasing with the Pd-Au electrode at the magnetic field on axis 0.3 T, the dependence of various parameters on the electrode position was experimentally determined. Figure 3 shows the radial profiles of the electron density n_e , the electron pressure $n_e T_e$ and the floating potential V_f measured with the triple probe, in configuration (b) at 0.3 T, where ρ was the normalized minor radius defined by $\rho = \langle r \rangle / a$, $\langle r \rangle$ was the average radius of the flux surface, and a was the average minor radius. The closed circles, closed squares, closed diamonds and closed triangles denote the kinetic

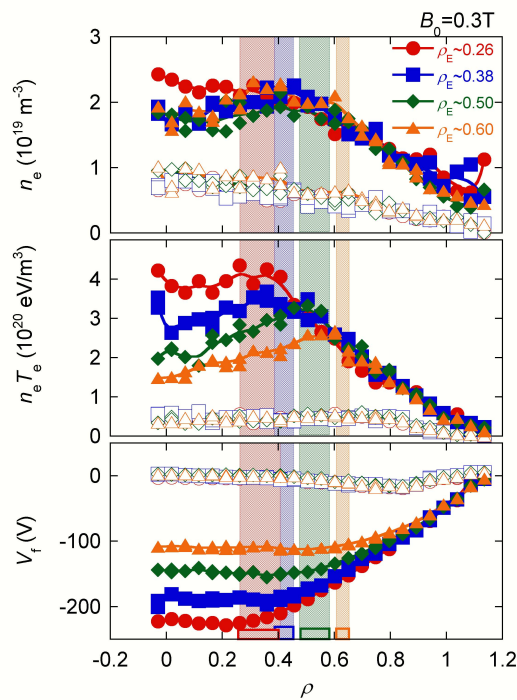


Fig. 3 Radial profiles of the electron density n_e , the electron pressure $n_e T_e$ and the floating potential V_f measured with the triple probe, in configuration (b) at 0.3 T.

pressure at the electrode head positions $\rho \sim 0.26, 0.38, 0.50,$ and 0.60 . The plasma profiles were changed by the change in the electrode position. The positions of the peak of n_e , $n_e T_e$, and V_f almost correspond to the electrode position. Large n_e , $n_e T_e$, and V_f gradients were formed by the insertion of the electrode near the center of plasma. The positions at which n_e , the $n_e T_e$ gradient, and E_r were formed almost correspond to the electrode position. This result shows that the more the electrode is inserted in plasma, the more the pressure rises; this is the effect of the particle supply by hydrogen injection from the electrode and the formation of a strong electric field by electrode biasing.

Experiments have been conducted using negative biasing with a stainless steel (SUS) electrode (cold electrode; ion collection) that had the same geometry and was inserted to the same position in the plasma. As a result, high-density plasma production was observed for only 4 discharges in one treatment for hydrogen storage. On the other hand, in negative biasing experiments with a Pd-Au electrode, the number of production of high-density plasma per hydrogen gas charge was over 30 times. It was estimated that the high-density plasma production in negative biasing experiments with the SUS electrode, which does not have a hydrogen storage capacity, is an effect of the hydrogen adsorbed with the oxide layer on the surface of the electrode, and the difference in the production of high-density plasma between SUS and Pd-Au electrodes is due to the amount of hydrogen storage. From these results, it was considered that the hydrogen in the electrode contributes to high-density plasma production. In negative biasing experiments with the SUS electrode, it is not easy to obtain a sufficient electrode current. On the other hand, in negative biasing experiments with a hot cathode electrode (electron-emitting), an increase of electron density and electron pressure and the formation of strong electric field were observed. However, the electron density and/or electron pressure by negative biasing with a hot cathode electrode was lower than that by negative biasing with hydrogen storage electrode. As described in the introduction, at TU-Heliac, the density increases when the injection gas pressure is raised, but it had not been confirmed that this pressure enhancement would occur in a hydrogen storage electrode biasing experiment. From the above-mentioned results, it was considered that the pressure increase was due to two effects: the particle supply by hydrogen injection from the electrode and the formation of strong electric field by electrode biasing.

In configuration (a), when the Pd-Au electrode was biased negatively at the magnetic field on axis 0.075 T, the electron density increased within a short time ($\Delta t \sim 0.5$ -1.0 ms). Figure 3 (a)-(d) shows the typical time evolution of the electrode voltage, V_E , electrode current, I_E , electron line-density, $n_e l$, and electron density, n_e at

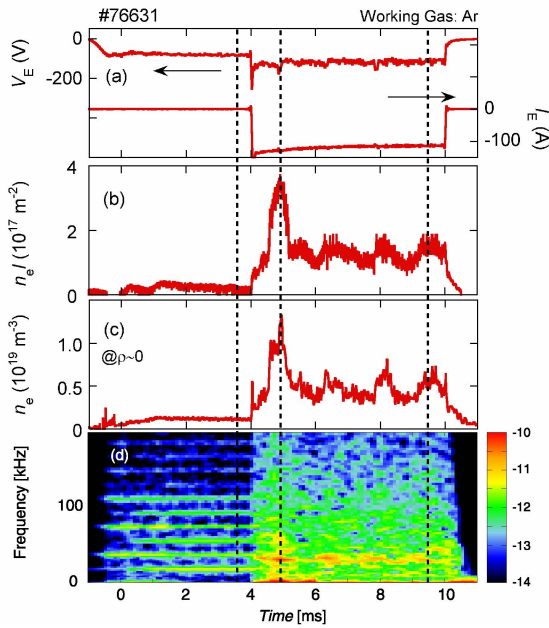


Fig. 4 The typical time evolution of (a) the electrode voltage, V_E , the electrode current, I_E , (b) the electron line-density, $n_e l$, (c) the electron density, n_e at $\rho \sim 0$, and (d) the power spectra calculated from the ion saturation current I_s obtained by the HSTP.

$\rho \sim 0$, and power spectra calculated from the ion saturation current I_s obtained by the HSTP. Fast Fourier transform was used in the calculation. When the Pd-Au electrode was biased negatively from 4 ms to 10 ms, the electrode current, I_E , increased up to about 100 A. This density increment was not sustained; after the density decrement smaller density increments were sometimes observed under electrode biasing. And, at the density increment phase, low-frequency ($f < 40$ kHz) fluctuations were observed. Such short-term high-pressure plasma discharge has been observed in configuration (c), but the duration of high-pressure plasma ($\Delta t < 0.5$ ms) was shorter than that in configuration (a).

Figure 5 shows the radial profiles of the electron pressure, $n_e T_e$, measured with the triple probe, in configuration (a) and configuration (c) at 0.075 T. The open triangles, closed triangles and closed circles denote the kinetic pressure at 3.5 ms (before biasing), at 9.5 ms (during biasing; after the density decrement), and at the $n_e l$ peak time (these times are indicated by broken lines in Fig. 3). In a few cases at configuration (a), though the electron pressure did not increase enough, the kinetic pressure at $n_e l$ peak time was about 5-fold compared with those before biasing, and about 2-fold compared with those during biasing (after the density decrement). On the other hand, in configuration (c), the kinetic pressure at $n_e l$ peak time was about 1.5-fold compared with those during

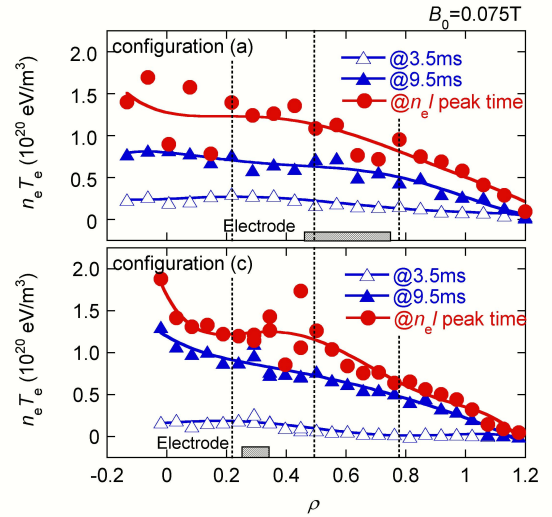


Fig. 5 The radial profiles of the electron pressure $n_e T_e$ measured with the triple probe, in configuration (a) and configuration (c) at 0.075 T. The open triangles, closed triangles and closed circles denote the kinetic pressure at 3.5 ms (before biasing), at 9.5 ms (during biasing; after the density decrement); and at the $n_e l$ peak time.

biasing (after the density decrement). Hence, the rate of increase and decrease were different between configuration (a) and configuration (c). In this experiment comparing different magnetic configurations, the electrode position in the magnetic hill configuration experiment was further inward than that in the magnetic well configuration experiment. However, while the pressure profiles were almost the same, the rate of increase and decrease were different between the well configuration and the hill configuration. It was considered that these results indicate that this increase is dependent on the magnetic configuration.

Figure 6 shows the time evolution of the local beta value β_{local} in configurations (a) and (c) at the magnetic fields on axis $B_0 = 0.3$ T, 0.150 T, and 0.075 T at $\rho \sim 0.77$. The β_{local} was defined as follows:

$$\beta_{\text{local}} = \frac{n_e k T_e}{B_0^2 / 2 \mu_0}, \quad (1)$$

where $n_e T_e$ was the local electron pressure, measured with a triple probe. In configuration (a), the local beta value β_{local} was totally higher than that in configuration (c). In configuration (a), when the short-term high-pressure plasma was produced, the local beta value β_{local} was the highest ($\beta_{\text{local}} \sim 0.7$ %), about 5-fold of those before biasing. In addition, the β_{local} value was about 1.5-fold of those during biasing (after the density decrement) and that in configuration (c) with electrode biasing.

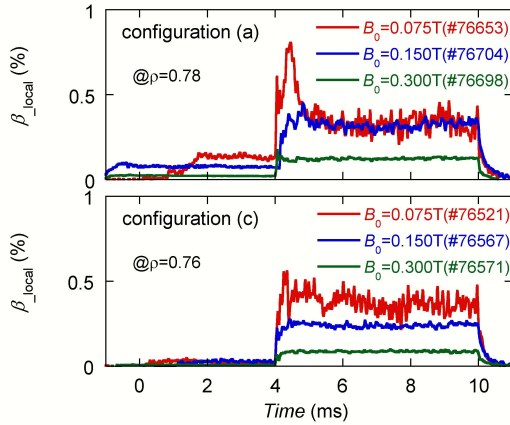


Fig. 6 The time evolution of the local beta value β_{local} in configurations (a) and (c) at the magnetic field on axis $B_0 = 0.3$ T, 0.150 T, and 0.075 T at $\rho \sim 0.77$.

Figure 7 shows the time evolution of the local beta value β_{local} in configurations (a) and (c) at the magnetic field on axis $B_0 = 0.075$ T at $\rho \sim 0.2$, 0.5 and 0.8, and power spectra were calculated from the ion saturation current I_s obtained by the HSTP. In configuration (a), when the local beta value β_{local} exceeded about 0.5 % ($\text{Time} = 4.2 \sim 4.6$ ms), the growth of low-frequency ($30 \text{ kHz} < f < 40 \text{ kHz}$) fluctuations was observed at each radial position. On the other hand, in configuration (c), the growth of fluctuations was not clearly observed at the same frequency. Furthermore, the power spectra were different in configurations (a) and (c) during biasing ($\text{Time} > 4.6$ ms) at each radial position. In configuration (c), low-frequency ($f = 18.8 \text{ kHz}$; ohmic heating frequency) fluctuations were observed, but in configuration (a), these fluctuations were suppressed. Consequently, these results suggest that the high-beta

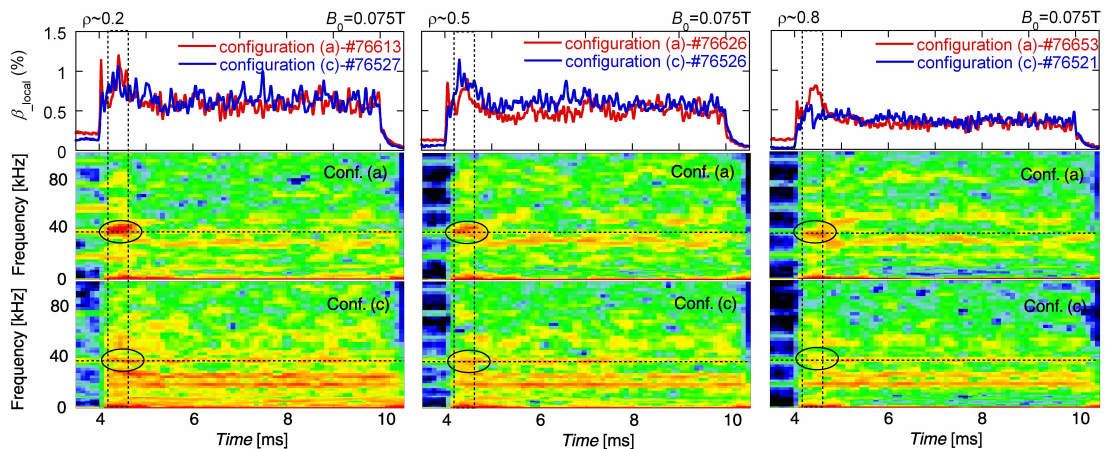


Fig. 7 The time evolution of the local beta value β_{local} in configurations (a) and (c) at the magnetic field on axis $B_0 = 0.075$ T at $\rho \sim 0.2$, 0.5, and 0.8, and power spectra were calculated from the ion saturation current I_s obtained by the HSTP.

plasma produced by the hydrogen storage electrode biasing depends on the magnetic configuration, and the degradation of high-beta plasma was triggered by MHD instability, caused by the rise of the beta value.

4. Summary

At TU-Heliac, high-pressure and high-beta discharge experiments were done with hydrogen storage electrode biasing by varying the magnetic configurations and the magnetic field. In standard configuration, by negative biasing with the Pd-Au electrode at the magnetic field on axis 0.3 T, the dependence of various parameters on the electrode position was experimentally determined. The results showed that the further the electrode is inserted into the plasma, the more the pressure rises; this is the effect of the particle supply by hydrogen injection from the electrode and the formation of a strong electric field by electrode biasing. In addition, a comparison of SUS electrode and hot cathode electrode biasing suggested that the pressure increase was due to two effects: the particle supply by hydrogen injection from the electrode and the formation of a strong electric field by electrode biasing.

High-beta plasma was produced in the magnetic well and hill configurations (magnetic well depths at the last closed flux surface (LCFS): 3.3 % and -1.6 %, respectively) at the magnetic field on axis $B_0 = 0.075$ T with hydrogen storage electrode biasing. The electron density increased at a short time range, and this density increment was degraded. In both magnetic well and hill configurations, this density increment was observed; however, the rate of increase and decrease were different between the well and hill configurations. When short-term high-pressure plasma was produced in the magnetic well configuration, the local beta value was the highest, about 5-fold of those before biasing. The

fluctuations of the ion saturation current observed at the electrode biasing were different in the well and hill configurations. Consequently, these results suggest that the high-beta plasma produced by hydrogen storage electrode biasing depends on the magnetic configuration, and the degradation of high-beta plasma was triggered by MHD instability, caused by the rise in the beta value.

5. Acknowledgments

This work was supported in part by the LHD Joint Planning Research program at the National Institute for Fusion Science and a grant-in-aid from the Ministry of Education, Science and Culture of Japan (No. 17360439) and a Research Fellowship of the Japan Society for the Promotion of Science for Young Scientist (No. 19-7419).

References

- [1] A. E. Bazhanova *et al.*, *Soviet-Phys. Tech. Phys.* **11** 1177 (1967).
- [2] S. Nagao *et al.*, *J. Phys. Soc. Jpn.* **27** 1082 (1969).
- [3] A. M. Mikhailovskii *et al.*, *Soviet. Phys. JEPT.* **39** 88 (1974).
- [4] S. Kitajima *et al.*, *J. Plasma Fusion Res. SERIES* **4**, 391 (2001).
- [5] S. Kitajima *et al.*, *Int. J. Appl. Electromagn. Mech.* **13** 381 (2002).
- [6] S. Kitajima *et al.*, *Nucl. Fusion* **46** 200 (2006).
- [7] H. Utoh *et al.*, *Proceedings of the 32nd EPS Conference on Plasma Physics* P2_066 (2005).
- [8] H. Utoh *et al.*, *Fusion Sci. Tech.* **50** 434 (2006).
- [9] H. Utoh *et al.*, *Journal of Physics: Conference Series* **123** 012024 (2008).
- [10] S. Kitajima *et al.*, *Japan. J. Appl. Phys.* **30** 2606 (1991).
- [11] T. Zama *et al.*, *Japan. J. Appl. Phys.* **32** 349 (1993).
- [12] Y. Tanaka *et al.*, *Plasma Fusion Res.* **2**, S1090 (2008).
- [13] Y. Tanaka *et al.*, *Plasma Fusion Res.* **3**, S1055 (2008).